



Universidad de Concepción
Dirección de Postgrado
Facultad de Ingeniería - Programa de Magister en Ciencias de la Ingeniería con
Mención en Ingeniería Civil

**Do obstacles in fishways enhance upstream passage for
non-sport fishes?**

**¿Los obstáculos en pasos de peces mejoran el paso aguas
arriba en peces no-deportivos?**

Tesis para optar al grado de Magister en Ciencias de la Ingeniería con
mención en Ingeniería Civil

CLAUDIA ALEJANDRA SANHUEZA CARRASCO
CONCEPCIÓN - CHILE
2016

Profesor Guía: Oscar Link Lazo
Dpto. de Ingeniería Civil, Facultad de Ingeniería
Universidad de Concepción

ABSTRACT

Chilean ichthyofauna has a high degree of endemism due to its evolution on a territory isolated by natural barriers. This scenario makes its protection essential to maintain native biodiversity. Moreover, Chile possesses a high hydroelectric potential which has generated the development of numerous hydropower plants. Each hydropower plant represents a physical barrier that fragments the river and disconnects fish's habitat. Fishways are the hydraulic structure designed to produce sustainable energy by reducing river's fragmentation but, in order to achieve an efficient fish passage, the turbulent flow produced should be favorable to the specific species, making imperative to understand how Chilean fishes relate with turbulence.

Research's objective is to describe and analyze the behavior of two endemic non-sport Chilean fish species (*Cheirodon galusdae* and *Basilichthys microlepidotus* juveniles) on an obstacle's wake, generated with a circular vertical cylinder in an open channel flow.

Wake vortices of vertical axis, were periodically shed as in the flow fields typically occurring in real nature-like fishways. Three experimental series with a total of seventy-two experiments were performed. Six individuals of each species were tested in free flow and in five different diameter cylinders. Two-dimensional Particle Image Velocimetry, PIV, was used to measure the flow at an horizontal plane. Wake vortices were described by their length-scale and frequency. Digital video of fish motion were analyzed to quantify tail beat amplitudes and frequencies.

Results show that both species interact differently with the wake. *C. galusdae* swam upstream escaping from vortices while *B. microlepidotus* kept its longitudinal position swimming on the wake. Tail beat amplitude, relative to fish length, increased with length-scale of the vortices and decreased with their frequency. Tail frequencies of *C. galusdae* increased with vortices length-scale and decreased with frequency. Tail frequencies of *B. microlepidotus* were constant in all experiments. Fish Strouhal number, correlated with vortex length-scale and fish length ratio for both species. It is concluded that wakes might serve as stimuli for upstream passage of *C. galusdae*. Additionally, *B. microlepidotus* would not favorable use cylinder wakes in a fishway and, compared to the undisturbed flow condition, it might exhibit higher energy consumption.

ACKNOWLEDGEMENTS

The financial support provided by the Chilean Research Council CONICYT through Grant FONDECYT 1150154: ‘Within-basin barriers and among-basin leaks: changing connectivity of rivers in central Chile and its impact on native fish’ is greatly acknowledged. So too is the support of HORIZON 2020 EU initiative through project ‘Knowledge Exchange for Efficient Passage of Fishes in the Southern Hemisphere’ (H2020-MSCA-RISE-2015-690857-KEEPFISH). EH and OL are supported by Red 14 Doctoral REDOC.CTA, MINEDUC project UCO1202 at U. of Concepción. Finally, many thanks go to Jorge González for his help in collecting fish, to René Iribarren for their collaboration during the experimental work, and to Karina Reyes, Daniela Baeza and Patricio Rubilar for their collaboration with the digital video-images analysis and processing.



CONTENTS

CHAPTER 1	INTRODUCTION.....	1
1.1	Motivation.....	1
1.2	Hypothesis.....	2
1.3	Objectives.....	2
1.4	Methodology.....	3
1.5	Structure of the thesis.....	4
CHAPTER 2	STATE OF THE ART REVIEW	5
2.1	Introduction	5
2.2	Background review	5
2.3	Conclusions	8
CHAPTER 3	EXPERIMENTAL SETUP.....	9
3.1	Introduction	9
3.2	Studied species	9
3.3	Experimental installation	11
3.4	Flow field	11
3.5	Fish motion.....	13
3.6	Experimental series.....	15
3.7	Velocity analysis.....	17
3.8	Conclusions	19
CHAPTER 4	FISH MOTION RESULTS.....	21
4.1	Introduction	21
4.2	Fish behavior	21
4.3	Tail beat amplitude, λ	22
4.4	Tail beat frequency, f_{TB}	23
4.5	Fish Strouhal number, St_{fish}	25
4.6	Discussion	26
4.7	Conclusions	28

CHAPTER 5 CONCLUSIONS 29
REFERENCES 30



LIST OF TABLES

Table 3.1 Experimental runs..... 16



LIST OF FIGURES

Figure 3.1	Endurance curves for <i>C. galusdae</i> and <i>B. microlepidotus</i>	10
Figure 3.2	Scheme of the experimental installation.....	11
Figure 3.3	Digitized points for determination of the tail beat amplitude λ	14
Figure 3.4	Mean velocity magnitude and normalized Reynolds stresses for experiment S3-19	17
Figure 3.5	Profiles of Turbulent Kinetic Energy along the centerline for experiments S3-1, S3-7, S3-13, S3-19 and S3-25	18
Figure 3.6	Calculated autocorrelation function and power spectral density for experiment S3-19.....	19
Figure 4.1	Pictures of a fish describing a typical trajectory in the cylinder wake.....	22
Figure 4.2	Normalized tail beat amplitude over relative vortex size and vortex frequency for experiments of series S2 and S3.....	23
Figure 4.3	Tail beat frequency, f_{TB} over relative vortex size and vortex frequency for experiments of series S2 and S3.....	24
Figure 4.4	Fish Strouhal number, St_{fish} over relative vortex size and vortex frequency for experiments of series S2 and S3.....	25

CHAPTER 1 INTRODUCTION

1.1 Motivation

Chile is a geographically isolated country, surrounded by the natural barriers of the Atacama Desert, Andes Mountains and Pacific Ocean. This natural condition produced an isolated development of fauna which caused a high degree of endemism on national ichthyofauna, meaning that a great quantity of native fish species cannot be found in any other place of the world and making its preservation an essential task. Also, to this limited natural scenario, it must be added the increasing development of artificial physical barriers caused by the construction of hydropower plants. Each hydropower plant represents a barrier that produces both river longitudinal fragmentation and disconnection of fish habitat.

Loss of physical connectivity is presumed to be one of the most generalized and important human induced alterations in riverine ecosystems, and it is frequently perceived as one of the main causes of the decline of freshwater fish species. Connectivity alterations produce different effects on different species, according to their dispersal abilities. Numerous fish species depend on connectivity along river systems to complete their life cycle and maintain genetic diversity and gene flow. Alternatively, species without distinctive migratory behavior may not suffer from such severe consequences of altered connectivity as migratory species do. However, over a long time period it is expected to produce loss of genetic diversity leading to a decline of fitness and possible extinction of the affected species.

In order to accomplish sustainable hydropower plants, longitudinal fragmentation of the river must be controlled. The technical alternative for mitigation of disconnection is the construction of fish-passes. Its hydraulic design requires basic information on fish swimming abilities like critical swimming speed and endurance, but also, recent studies have shown the important role of turbulence features like turbulent kinetic energy, and the presence of burst and sweep events in the wake of boulders. The effects of vortices on swimming abilities of rainbow trout have been explored, showing that vortices can be attractive or repulsive to fishes depending on their relative size to fish length. These effects should be taken into account on fishway design.

So far, the existent information on fish swimming has been developed for northern species with natural high swimming capacities, but for most of the non-sport freshwater fish species it is scarce or non-existent. Generation of new antecedents on fish swimming abilities of non-sport fishes might be helpful to find out if existent design guidelines for fishways are applicable to them and, if not, which special considerations should be made to achieve an efficient non-sport multispecies fishway design.

1.2 Hypothesis

Non-sport fishes interact with wake vortices and thus modify their swimming modes in a manner that these vortices could be used for provision of stimuli for the upstream passage.

1.3 Objectives

1.3.1 General objective

The general objective was to describe and analyze the behavior of two species of non-sport Chilean fish in the wake of vortices produced by an obstacle in the flow.

1.3.2 Specific objectives

In order to accomplish the research objective, the following tasks were defined:

- a) Assess the experimental design to define: target fish species, parameters to measure, trial settings and measurement technique to both flow and fish.
- b) Assemble the physical installation to measure flow and fish swimming in the laboratory.

- c) Measure the flow field using Particle Image Velocimetry (PIV) and, measure the fish motion by video recording.
- d) Characterize the flow and fish swimming through the chosen parameters.
- e) Analyze the effect of flow turbulence on fish's behavior.

1.4 Methodology

A background review about the influence of turbulence on fish swimming was realized to identify the parameters of interest to be measured during the experiments, and also to define the experimental setup and series configuration required to be recreated on laboratory.

Two species of Chilean non-sport fish were chosen to be studied, *Cheirodon galusdae* and *Basilichthys microlepidotus*, according to their future threats, swimming characteristics (subcarangiform and carangiform, respectively) and conservation status (both designated as *Vulnerable* according to Vila and Habit, 2015).

The experimental series was defined based on the swimming capacities of fishes, this means that water velocity was established so fishes were able to swim for long time periods without reaching fatigue. Six individuals of each species were tested with free flow and then with five different diameter circular cylinders, meaning a total of 72 experiments.

Two-dimensional Particle Image Velocimetry (PIV) was the technique chosen to measure flow characteristics. PIV consists on incorporate small tracer particles to the flow, they were then illuminated using a plane of light and their motion was recorded with a camera. The recorded videos were processed to identify the motion and displacement of groups of particles by using cross correlation between two sequential frames. Once the displacements were calculated, and knowing the time elapsed between frames, the velocity field was calculated. The information given by the velocity field was post-processed to describe flow and vortex characteristics.

To describe fish motion, fishes were recorded while swimming on the flume's installation and then the videos were analyzed with two different techniques. First, to describe fish behavior, image processing was used by converting the gray images of fish on the flume to binary images and evaluating the characteristics of the area corresponding to fish body, this was made for lapses of time long enough to register a representative performance of the fish based on the general behavior observations. Secondly, to describe changes on swimming mode, amplitude and frequency of the tail were digitized in free flow and in the presence of wake vortices.

Finally, to analyze the effect of turbulence on fish swimming, the results of flow and fish motion characteristics were plotted on a dimensionless way, allowing comparison of the results between the two different species. The tendencies observed on the graphs were analyzed and the discussion about the implications of the results on the design of fishways is presented.

1.5 Structure of the thesis

In Chapter 1 the global research problem is defined, the motivation, working hypothesis, objectives and methodology are presented. Chapter 2 presents a review of the state of the art related with fish motion, flow analysis and the interaction between these topics to be used on fishways design. Chapter 3 describes the experimental setup installed in the laboratory of Hydraulic and Environmental Engineering at the University of Concepción, this includes; fish species description, measurement techniques, experimental installation and series configuration. Chapter 4 presents the results of fish behavior on the wake and the relation between tail's amplitude and frequency with vortices length-scale and frequency. Discussion of the results is also included. Finally, in Chapter 5 research's conclusions are presented.

CHAPTER 2 STATE OF THE ART REVIEW

2.1 Introduction

Important research decisions were taken supported by a background review of the fundamental investigations related with fish performance, flow measurement and the effects of turbulence on fish motion. The results of the background review are presented below.

It is important to highlight that topics here presented were chosen with the aim of study the details of this particular thesis, and so, some information considered as least relevant for this specific task, has been omitted.

2.2 Background review

The decline of freshwater fish biodiversity is occurring at an alarming and persistent rate. Given that most fish must undertake some form of migration to complete their life-cycle, the high proliferation of hydropower schemes is of particular concern. It has been shown that hydropower facilities and other hydraulic structures, such as weirs and culverts, block migration routes, and assessment of the associated impacts on fish populations are especially complex in regions with diverse and poorly understood fish stocks (Castro-Santos *et al.*, 2009; Zarfl *et al.*, 2015; Link and Habit, 2015). Several locations in the southern hemisphere are among the major global hotspots of hydropower development, however at the same time, they host some of the least studied ‘non-sport’ fish communities in the world (Laborde *et al.*, 2016). Mitigation action through fish passages have been proposed to avoid critical impacts. However, one of the greatest challenges in fish passage technology is the development of structures and design concepts suitable for a broad range of species (Castro-Santos *et al.*, 2009). Due to this, the EU Water Framework Directive 2000/60/EC is actively encouraging the development of fish passage (and screening) criteria for multiple species throughout their life history (Russon and Kemp, 2011).

The reasons explaining why some fishways work better than others and why some species perform better than others in particular fishways are still poorly understood (Castro-Santos *et al.*, 2009). Some of the variables that could affect fish passage in a fishway include (Goettel *et al.*, 2015; Link and Habit, 2015): (1) biological characteristics, as for instance the migration and movement patterns, body size, swimming and non-swimming modes, sensitive properties like olfactory orientation, acoustic sensibility and circadian rhythms; (2) ecological characteristics, such as habitat and food preferences, light intensity and water temperature, behavior in the hydraulic environment, presence of conspecifics and predators; and (3) hydraulic properties of the fishway, e.g., geometry, substrate and vegetation, length, slope, flow depth, velocity and turbulence level.

Fish swimming performance in a free flow can be related to the swimming speeds, fish size, tail beat frequency, and, to a lesser extent, to the tail beat amplitude (Bainbridge, 1958; Hunter and Zweifel, 1971; Videler and Wardle, 1991). In this context, previous studies have shown evidence on the relation between the flow structure and energy consumption (Enders *et al.*, 2003; Lupandin, 2005). The simplest way to represent the level of turbulence in a flow is through the flow Reynolds number, Re . Other time-averaged turbulence characteristics such as Reynolds stresses, Turbulent Kinetic Energy, etc., commonly scale with Re . Nikora *et al.* (2003) found negligible effects of turbulence created by wavy walls on swimming ability of puye (or inanga) *Galaxius maculatus*, while Enders *et al.* (2003) found that turbulence increase energy consumption of juvenile Atlantic salmon *Salmo salar*. Lupandin (2005) studied the effects of grid turbulence on perch *Perca fluviatilis*, finding that relative vortex size affects the fish balance, and the torque generated by the hydrodynamic forces favors fish overturn. In order to stabilize their position, the fish spreads its pectoral fins, which increases their hydraulic resistance and consequently decreases the swimming speed. Forces imparted onto fish from eddies can potentially modify fish swimming rates, forcing them to accelerate in particular areas. Also these forces may affect the fish position and balance, and can cause a fish to decrease its speed or to become disoriented (Dermisis and Papanicolaou, 2009). Fish also may expend extra energy when swimming through turbulent regions, especially if there is non-periodicity in the turbulence (Lacey *et al.*, 2012). Turbulence induced by geometry, like wakes, can be substantially different than that observed in the free flow case.

Wakes can be generated in a fishway through bluff bodies placed in the flow. Wakes are typically found in the so-called shear-layer transition regime which occurs in the range $1000 < Re_D < 200.000$ (Williamson, 1996). The Cylinder Reynolds number is defined as $Re_D = \rho UD/\mu$, where ρ is the fluid density, U the section averaged velocity, D the cylinder diameter and μ the dynamic viscosity of water. Under these conditions the vortices are developed by means of a shear layer characterized by two-dimensional instabilities of the Kelvin-Helmholtz type (Fey *et al.*, 1998). These wake vortices of vertical axis are shed periodically. Shao *et al.* (2010) studied the hydrodynamic performance of a fishlike undulating foil in the wake of a D-section cylinder through numerical simulations. They observed that when an undulating foil was placed at different distances behind the D-section cylinder, different wake structures are formed. The wake area was divided into three domains sub-areas: suction domain, thrust enhancing domain, and weak influence domain. Undulation played a negative role in propulsion when the foil was located near the cylinder (largely in the suction domain) and a positive role when the distance between the foil and the cylinder was beyond a critical value. The foil bypassing the vortices undergone both minimum thrust and input power, whereas the one passing through vortices experienced larger thrust.

Tritico and Cotel (2010) studied the effects of turbulent vortices caused by vertical and horizontal cylinders on the stability and critical swimming speed of *Semotilus atromaculatus*, finding that swimming stability is more sensible to horizontal eddies, and that critical swimming speed decrease with the presence of eddies. In special circumstances, however, it has been shown that turbulence may allow fish to harness energy from the flow to enhance their swimming performance (Liao *et al.*, 2003a; Liao *et al.* 2003b; Liao, 2007; Taguchi and Liao, 2011). Fish behavior in wakes is species-specific and thus obstacles in the flow as fishway elements, such as cylinders and boulders, may or not generate attraction flow, stimuli for upstream passage, resting areas, and/or behavioral barriers. Intensity, periodicity, orientation and size of wake vortices are expected to control fish behavior and swimming performance since they are critical for fish maneuvering and swimming stability (Lacey *et al.*, 2012; Maia *et al.*, 2015).

2.3 Conclusions

Based on the antecedents here presented and, in order to explore conditions under which obstacles in fishways enhance upstream passage of different non-sport fishes, we decided to study the behavior and tail beat kinematics of two species observing its dependence to vortex length-scale (size) and periodicity (frequency) in a cylinder wake. These decisions were taken with the aim of contribute to the development of design criteria for multispecies fishways.



CHAPTER 3 EXPERIMENTAL SETUP

3.1 Introduction

This chapter describes the experimental installation developed to measure the characteristics of flow and fish motion on the wake of a circular cylinder in an open channel flow. In order to accomplish this, the description of studied species, flume circuit, flow measurement technique, fish behavior measurement technique and experimental series configuration are presented.

3.2 Studied species

Two species of Chilean non-sport fish (*Cheirodon galusdae* and *Basilichthys microlepidotus*) were chosen to be studied according to their future threats, conservation status and swimming characteristics. The studied species are endemic to the Chilean ichthyogeographic province (Dyer, 2000) which is a region classified as a biodiversity hotspot (Myers *et al.*, 2000) and with a high pressure for hydropower development with about 1000 new expected projects of small hydropower plants (Ministerio de Energía, 2015) representing a threat to their future conservation.

Cheirodon galusdae inhabits at the piedmont of the Andes and Central Valley from 35 to 39° Lat. S. (Dyer, 2000). Maximum body size is 90 mm when adult, swimming mode is subcarangiform. *Basilichthys microlepidotus* inhabits at the piedmont of the Andes and Central Valley from 21 to 40° Lat. S. (Véliz *et al.*, 2012). Maximum body size is 120 mm for juveniles and 300 mm when adults. Swimming mode is carangiform (Link and Habit, 2015). Conservation status of both species is Vulnerable (Vila and Habit, 2015). Endurance was described for both species by Laborde *et al.* (2016) as shown in Figure 3.1.

It is expected that species with different swimming modes contribute to understand in a more integrated way the requirements on a multispecies fishway. However, it is important to mention that size of individuals was limited by experimental instruments to 150 mm and so, *C. galusdae* were represented with adults and *B. microlepidotus* only with juveniles.

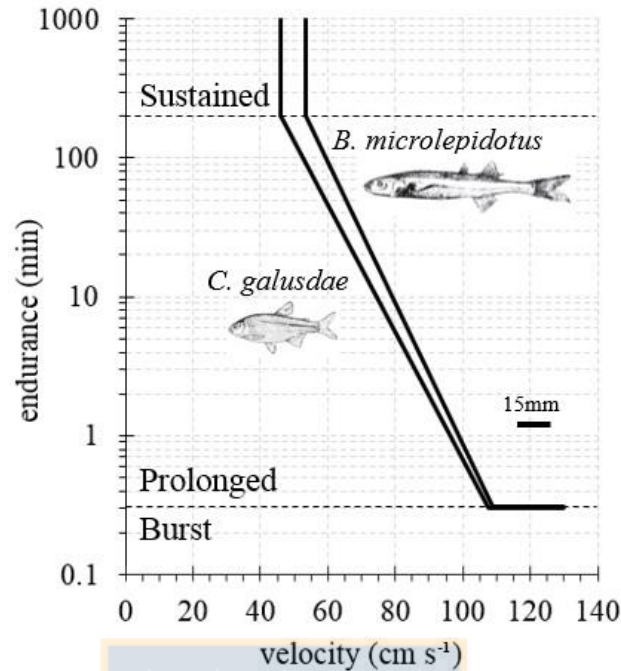


Figure 3.1 Endurance curves for *C. galusdae* and *B. microlepidotus* (after Laborde *et al.*, 2016)

Fish were collected from the Itata River using a backpack electroshocker (Smith-Root LR24, Vancouver, WA, USA) and seine net (2-mm mesh). All collected fish were transported to glass aquariums at the Hydraulics and Environmental Engineering Laboratory of the University of Concepción. To avoid mortality, guidelines for fish transportation and successful maintenance in captivity of Chilean native fish were followed (Sobenes *et al.*, 2012). Fish were kept for at least 15 days before experiments. Fish were fed *ad libitum* with live prey (macroinvertebrates from streams and *Enchitrea* sp., *Tenebrio molitor*, and *Eisenia foetida*) three or four times a week according to Sobenes *et al.* (2012) and García *et al.* (2012). Following Jobling (1982), feeding was interrupted 48 h before each experiment. Water temperature was kept stable at $17 \pm 1^\circ\text{C}$ for 1 week before the experiment. A total of 12 individuals (6 *C. galusdae* and 6 *B. microlepidotus*) of similar body length (44.8 ± 1.5 mm for *C. galusdae* and 77.7 ± 5.9 mm for *B. microlepidotus*) were tested.

3.3 Experimental installation

Experiments were conducted in a laboratory flume with 6 m length, 40 cm width, and 40 cm height located at the Hydraulics and Environmental Engineering Laboratory of the University of Concepción. A honeycomb matrix was placed at the flume entrance to provide a smooth flow. A measuring section of 0.65 m length, located 2.5 m downstream from the entrance was isolated with a net in order to keep fishes in the interrogation area. Vertical mounted cylinders with diameters of 2, 3, 4, 5 and 6 cm were placed at the upstream end of the test section. The discharge was controlled by a variable frequency drive and measured with an electromagnetic flow meter having an accuracy of $\pm 0.5\%$. The flow depth was controlled by adjusting the tail gate at the end of the flume, and was measured with ultrasonic distance sensors (UDS) placed along the flume. Figure 3.2 shows the experimental installation schematically.

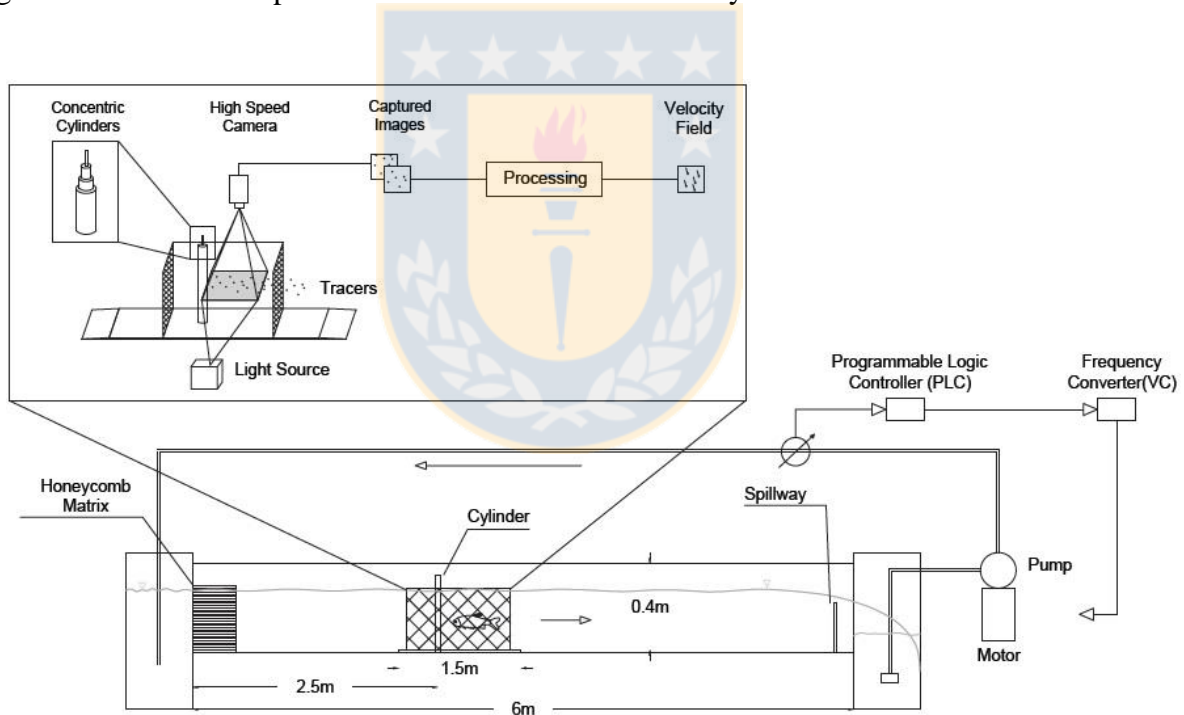


Figure 3.2 Scheme of the experimental installation

3.4 Flow field

The presence of the cylinder in the flow resulted in the development of a turbulent wake. This flow structure was characterized using a two dimensional Particle Image Velocimetry (PIV)

measurement system. Its principle is simple, small tracer particles are added to the flow, they are illuminated using a plane of light and their motion recorded with a camera. In PIV the motion of groups of particles are estimated by determining their displacement, Δx , in two sequential frames, which occur after Δt s. Since the displacement and time are known the velocity can be estimated. The accuracy of the estimation depends on the physical and optical properties of the particles. In this work Polyamide-12 particles of 100 μm diameter and 1.06 g/cm^3 density were used. The size and density of these particles ensure that they will respond to a wide range of flow structures of interest (Melling, 1997). The particles material and white color allow a high performance scattering of the light source. As standard in PIV, the displacements were determined by calculating the correlation between interrogation areas via Fourier Transform. These displacements were calculated using the toolbox for Matlab, PIVlab® developed by Thielicke and Stamhuis (2014a) in its version Thielicke and Stamhuis (2014b). A multi-pass approach with final interrogation windows of 32 x 32 Pix was used for the calculations. With the aim of improving the velocity estimation in high shear regions, the image deformation technique was used (Scarano, 2001). The displacements calculation was improved using a Gaussian subpixel accuracy estimation (Adrian and Westerweel, 2011).

The particles seeding density was carefully designed to allow the recommended minimum of ~5 particles in each interrogation windows (Adrian and Westerweel, 2011). A Sony Action Cam HDR-AS100V® with a 32GB memory, 1280x720 pix resolution and acquisition frequency of 120 Hz was used to record the particles motion. For the flow conditions analyzed, the 120 Hz allowed displacements between frames larger than the particles diameter in the images, thus errors produce by short displacements were minimized. These displacements were also long enough to allow a good correlation peak magnitude in the correlation analysis.

An enclosure around the flume was built to avoid the recording of environmental light in the images. Analogously to the work by Gross *et al* (2010) two sources of light were used as the light density of a single one was not enough to produce a good contrast level in the images. The light was collimated to illuminate a flow region of 20 cm-long and 0.8 cm-wide. According to Gross *et al*. (2010) the use of the collimated light has a minimal divergence thus it can reliably be used for PIV measurements.

Before the measurements, but using same experimental conditions, a target containing reference marks was placed in the flow channel at same position as the light plane. Images of the target were used to correct the PIV images for typical barrel and pincushion lens distortions, but also to correct optical deformations induced by the experimental setup. After the PIV processing was completed, the displacements in camera coordinates (pix) were converted to real world coordinates (cm) using also the information provided by the calibration target.

Even under the most carefully controlled laboratory environment, outlier vectors will be generated in the PIV analysis. In case of the present study, the percentage of outliers in individual frames was always less than the 4~5 % recommended (Adrian and Westerweel, 2011). During the post processing of the estimated velocity fields, the universal outlier filter of Westerweel and Scarano (2005) was used for outliers removal, while a cubic interpolation technique was used for their estimation.

The flow field was measured at a horizontal plane located at a height of 40% of the flow depth. To ensure statistical convergence, the flow field was measured during 7 minutes, *i.e.*, 50400 frames.

In the experiments cylinder wakes were in the shear-layer transition regime (Williamson, 1996) with Kelvin-Helmholtz instabilities (Schlichting and Gersten, 1997; Fey *et al.*, 1998). The observed relationship between Re_D and St followed the curve proposed by Fey *et al.* (1998):

$$St = \begin{cases} 0.2040 + \frac{0.3364}{\sqrt{Re_D}} & 1300 < Re_D < 5000 \\ 0.1776 + \frac{2.2023}{\sqrt{Re_D}} & 5000 < Re_D < 2 \cdot 10^5 \end{cases}, \quad (3.1)$$

3.5 Fish motion

Video records of fish motion, with 20 minute duration for each cylinder plus free flow condition, totaling 120 minutes of performance per fish, were analyzed to characterize the fish behavior

and the tail beat kinematics. Fish were recorded dorsally at 120 fps using a Sony Action Cam HDR-AS100V®. The images obtained with this camera were also corrected from optical distortions.

3.5.1 Fish behavior

The behavior of fish, measured as fish position in the flume while confronting the vortices in the wake, was interpreted from recorded fish trajectories. This was achieved through the development of a MATLAB® script for the processing of the videos. The intensity of the gray scale images was inverted and binarized using the thresholding method proposed by Otsu (1979). After this, the centroid of the fish was calculated in the individual binary frames and the trajectories tracked. This information was used to obtain the probability density function of the vertical and horizontal fish position.

3.5.2 Tail beat kinematics

Tail beat amplitude and tail beat frequency were determined following the methodology by Oufiero *et al.* (2014). Videos were digitized using the software ImageJ (U.S. National Institutes of Health, Bethesda, Maryland, USA, <http://imagej.nih.gov/ij/>). The base of the caudal fin was digitized for 30 full tail beats taken from portions of the swim trails with minimal movement of the fish. This point was digitized when the tail was extended maximally laterally, on either side for each of the 30 full tail beats (Figure 3.3).

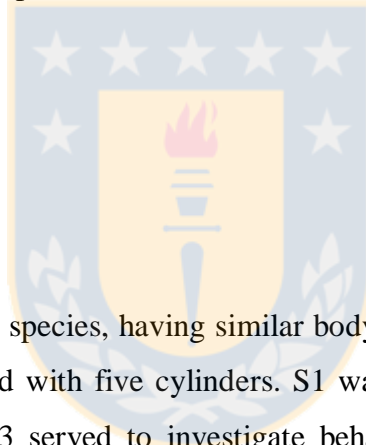


Figure 3.3 Digitized points for determination of the tail beat amplitude λ

Horizontal and vertical coordinates for each video and trial were further processed to obtain the average tail beat amplitude and timing, averaged over the 30 tail beats. As shown in Figure 3.3,

the tail amplitude was defined as the average distance between points 1 and 2, which represent the maximum lateral extension of the caudal fin from the right to the left side of the fish. Tail beat time was the time it took for one complete tail beat cycle, from maximal lateral position on the right side of the fish, through the center position, to the maximum lateral position on the left side of the fish, and back to the original starting position on the maximum lateral right side. From these two traits, tail beat frequency was calculated, *i.e.* the inverse of the tail beat time was calculated, giving an estimate of the number of tail beats per second.

It is important to highlight that *C. galusdae* use the swimming style burst-and-coast, a movement pattern consisting of propulsion phases alternated with ‘resting’ phases where the fish does not move neither its body nor its tail. Instead, *B. microlepidotus* present a fluid swimming movement. This means that frequency here presented includes the ‘resting’ lapses for *C. galusdae* but not to *B. microlepidotus*.



3.6 Experimental series

Six individuals of each studied species, having similar body length and critical swimming speed, were tested with free flow, and with five cylinders. S1 was the reference series with free flow experiments. Series S2 and S3 served to investigate behavior and tail beat kinematics of *C. galusdae* and *B. microlepidotus*, respectively. These three series totalized 72 experiments. Table 3.1 summarizes conditions for each experiment.

In all experiments the section averaged flow velocity was equal 0.7 times the critical swimming speed of the individual, which was determined by Laborde *et al.* (2016). Each trial began with 1.5 hours of acclimatization with a section averaged velocity of 1 BL/s in order to decrease the stress produced on the fish. Subsequently, flow velocity was slowly raised up to the tested condition ($U = 0.7U_{cr}$). The experiments spanned cylinder Reynolds number ($Re_D = \rho UD/\mu$, where ρ is the fluid density, U the section averaged velocity, D the cylinder diameter and μ the dynamic viscosity) in the range of 3000 to 17000 and flow Strouhal number ($St = fD/U$, where f is the shedding frequency) from 0.17 to 0.21.

Table 3.1 Experimental runs

Series	Number	L (cm)	Uc (m/s)	U (m/s)	H (m)	D (m)	f (Hz)	λ (cm)	f_{TB} (Hz)	D* (=D/L)	Re _D (=UD/v)	St (=fD/U)	λ^* (= λ/L)	St _{Fish} (= $f_{TB} L/U$)
S1 (free flow)	1	4.3	0.33	0.23	0.24	-	-	0.95	7.91	-	-	-	0.22	0.343
	2	4.3	0.30	0.21	0.30	-	-	1.15	8.42	-	-	-	0.27	0.450
	3	4.5	0.31	0.22	0.30	-	-	1.18	7.41	-	-	-	0.26	0.405
	4	4.5	0.32	0.23	0.28	-	-	1.07	5.92	-	-	-	0.24	0.289
	5	4.6	0.31	0.22	0.25	-	-	1.21	6.84	-	-	-	0.26	0.390
	6	4.7	0.32	0.23	0.30	-	-	1.44	6.52	-	-	-	0.31	0.446
	7	7.2	0.21	0.15	0.25	-	-	1.51	5.37	-	-	-	0.21	0.499
	8	7.2	0.23	0.16	0.27	-	-	1.41	5.48	-	-	-	0.20	0.477
	9	7.6	0.26	0.18	0.28	-	-	1.60	4.18	-	-	-	0.21	0.367
	10	7.7	0.28	0.20	0.24	-	-	1.23	4.94	-	-	-	0.16	0.314
	11	8.0	0.30	0.21	0.24	-	-	1.20	4.00	-	-	-	0.15	0.236
	12	8.9	0.37	0.26	0.23	-	-	1.47	4.86	-	-	-	0.16	0.285
S2 (<i>C. galusdae</i>)	1	4.3	0.33	0.23	0.24	0.02	2.46	1.06	7.86	0.47	4962	0.198	0.25	0.407
	2	4.3	0.30	0.21	0.30	0.02	1.99	1.20	8.42	0.47	4508	0.177	0.28	0.510
	3	4.5	0.31	0.22	0.30	0.02	2.34	1.19	7.41	0.44	4611	0.203	0.26	0.464
	4	4.5	0.32	0.23	0.28	0.02	2.34	1.15	5.92	0.44	4887	0.192	0.26	0.341
	5	4.6	0.31	0.22	0.25	0.02	2.29	1.19	7.67	0.43	4643	0.197	0.26	0.428
	6	4.7	0.32	0.23	0.30	0.02	2.40	1.15	6.48	0.43	4829	0.199	0.25	0.370
	7	4.3	0.33	0.23	0.24	0.03	1.52	1.08	9.84	0.70	7442	0.184	0.25	0.492
	8	4.3	0.30	0.21	0.30	0.03	1.29	1.20	8.95	0.70	6761	0.172	0.28	0.533
	9	4.5	0.31	0.22	0.30	0.03	1.52	1.16	8.58	0.67	6917	0.198	0.26	0.506
	10	4.5	0.32	0.23	0.28	0.03	1.64	1.09	6.54	0.67	7330	0.201	0.24	0.360
	11	4.6	0.31	0.22	0.25	0.03	1.52	1.23	8.10	0.65	6965	0.197	0.27	0.448
	12	4.7	0.32	0.23	0.30	0.03	1.58	1.15	9.40	0.64	7243	0.197	0.24	0.508
	13	4.3	0.33	0.23	0.24	0.04	1.23	1.07	8.48	0.93	9923	0.198	0.25	0.408
	14	4.3	0.30	0.21	0.30	0.04	0.94	1.19	9.70	0.93	9015	0.166	0.28	0.565
	15	4.5	0.31	0.22	0.30	0.04	1.23	1.35	10.01	0.89	9223	0.213	0.30	0.479
	16	4.5	0.32	0.23	0.28	0.04	1.17	1.50	7.27	0.89	9773	0.192	0.33	0.409
	17	4.6	0.31	0.22	0.25	0.04	1.17	1.34	7.81	0.87	9287	0.202	0.29	0.480
	18	4.7	0.32	0.23	0.30	0.04	1.17	1.44	8.41	0.85	9658	0.194	0.31	0.561
	19	4.3	0.33	0.23	0.24	0.05	1.00	1.09	9.84	1.16	12404	0.201	0.25	0.481
	20	4.3	0.30	0.21	0.30	0.05	0.82	1.28	10.32	1.16	11269	0.182	0.30	0.647
	21	4.5	0.31	0.22	0.30	0.05	0.94	1.32	7.93	1.11	11528	0.203	0.29	0.444
	22	4.5	0.32	0.23	0.28	0.05	1.00	1.52	6.00	1.11	12216	0.204	0.34	0.621
	23	4.6	0.31	0.22	0.25	0.05	1.00	1.34	8.68	1.09	11609	0.215	0.29	0.534
	24	4.7	0.32	0.23	0.30	0.05	0.94	1.47	9.10	1.06	12072	0.194	0.31	0.615
	25	4.3	0.33	0.23	0.24	0.06	0.88	1.16	8.34	1.40	14885	0.213	0.27	0.436
	26	4.3	0.30	0.21	0.30	0.06	0.70	1.33	10.95	1.40	13523	0.187	0.31	0.576
	27	4.5	0.31	0.22	0.30	0.06	0.82	1.24	7.48	1.33	13834	0.213	0.28	0.383
	28	4.5	0.32	0.23	0.28	0.06	0.82	1.65	9.00	1.33	14660	0.201	0.37	0.596
	29	4.6	0.31	0.22	0.25	0.06	0.82	1.42	7.37	1.30	13930	0.212	0.31	0.482
	30	4.7	0.32	0.23	0.30	0.06	0.82	1.75	9.90	1.28	14487	0.204	0.37	0.798
S3 (<i>B. microlepidotus</i>)	1	7.2	0.21	0.15	0.25	0.02	1.64	1.58	4.88	0.28	3223	0.204	0.22	0.473
	2	7.2	0.23	0.16	0.27	0.02	1.82	1.65	5.09	0.28	3669	0.198	0.23	0.518
	3	7.6	0.26	0.18	0.28	0.02	1.88	1.53	4.36	0.26	4059	0.185	0.20	0.367
	4	7.7	0.28	0.20	0.24	0.02	1.99	1.40	5.04	0.26	4385	0.182	0.18	0.369
	5	8.0	0.30	0.21	0.24	0.02	1.99	1.28	4.44	0.25	4545	0.175	0.16	0.279
	6	8.9	0.37	0.26	0.23	0.02	2.46	1.62	5.44	0.22	5652	0.174	0.18	0.353
	7	7.2	0.21	0.15	0.25	0.03	1.11	1.72	5.04	0.42	4835	0.207	0.24	0.540
	8	7.2	0.23	0.16	0.27	0.03	1.17	1.65	5.21	0.42	5504	0.192	0.23	0.530
	9	7.6	0.26	0.18	0.28	0.03	1.29	1.77	4.32	0.39	6088	0.191	0.23	0.424
	10	7.7	0.28	0.20	0.24	0.03	1.29	1.55	5.00	0.39	6577	0.176	0.20	0.407
	11	8.0	0.30	0.21	0.24	0.03	1.41	1.68	4.27	0.38	6817	0.186	0.21	0.353
	12	8.9	0.37	0.26	0.23	0.03	1.70	1.51	5.13	0.34	8478	0.180	0.17	0.310
	13	7.2	0.21	0.15	0.25	0.04	0.88	1.89	5.00	0.56	6447	0.218	0.26	0.588
	14	7.2	0.23	0.16	0.27	0.04	0.88	1.89	5.29	0.56	7338	0.192	0.26	0.617
	15	7.6	0.26	0.18	0.28	0.04	1.00	1.72	4.62	0.53	8117	0.196	0.23	0.436
	16	7.7	0.28	0.20	0.24	0.04	1.06	1.77	4.83	0.52	8770	0.192	0.23	0.447
	17	8.0	0.30	0.21	0.24	0.04	1.11	1.53	4.65	0.50	9090	0.196	0.19	0.349
	18	8.9	0.37	0.26	0.23	0.04	1.35	1.56	4.51	0.45	11303	0.191	0.17	0.281
	19	7.2	0.21	0.15	0.25	0.05	0.70	1.87	5.03	0.69	8059	0.218	0.26	0.582
	20	7.2	0.23	0.16	0.27	0.05	0.76	1.73	5.48	0.69	9173	0.208	0.24	0.584
	21	7.6	0.26	0.18	0.28	0.05	0.82	1.71	4.67	0.66	10146	0.202	0.23	0.440
	22	7.7	0.28	0.20	0.24	0.05	0.88	1.62	4.96	0.65	10962	0.200	0.21	0.421
	23	8.0	0.30	0.21	0.24	0.05	0.88	1.58	4.40	0.63	11362	0.193	0.20	0.339
	24	8.9	0.37	0.26	0.23	0.05	1.06	1.85	4.66	0.56	14129	0.187	0.21	0.332
	25	7.2	0.21	0.15	0.25	0.06	0.59	1.91	5.67	0.83	9670	0.218	0.26	0.663
	26	7.2	0.23	0.16	0.27	0.06	0.64	1.96	5.43	0.83	11007	0.211	0.27	0.655
	27	7.6	0.26	0.18	0.28	0.06	0.70	1.93	4.78	0.79	12176	0.208	0.25	0.508
	28	7.7	0.28	0.20	0.24	0.06	0.76	1.86	4.98	0.78	13155	0.208	0.24	0.484
	29	8.0	0.30	0.21	0.24	0.06	0.76	1.62	4.64	0.75	13635	0.201	0.20	0.369
	30	8.9	0.37	0.26	0.23	0.06	0.94	1.85	4.95	0.67	16955	0.199	0.21	0.350

3.7 Velocity analysis

The instantaneous longitudinal and spanwise velocity components were defined as $u(x, y)$ and $v(x, y)$, respectively. Following the Reynolds decomposition, the time-averaged components and fluctuating part of the velocity, in these directions, can be defined as equations 3.2 and 3.3.

$$u(x, t) = \bar{u}(x) + u'(x, t), \quad (3.2)$$

$$v(x, t) = \bar{v}(x) + v'(x, t), \quad (3.3)$$

Based in these definitions it is possible to introduce the Reynolds Stress Tensor, which summarizes some of the time averaged turbulence characteristics of the flow. Assuming a mainly two-dimensional flow, the tensor can be defined as equation 3.4.

$$\tau' = \rho \begin{bmatrix} \overline{u'u'} & \overline{u'v'} \\ \overline{v'u'} & \overline{v'v'} \end{bmatrix}, \quad (3.4)$$

Due to the symmetry properties of the tensor (Tennekes and Lumley, 1972), the off-diagonal shear stress components are equal, *i.e.* $\overline{u'v'} = \overline{v'u'}$. An example of the measured mean velocity magnitude, $\sqrt{\bar{u}^2 + \bar{v}^2}$, and normalized Reynolds stress, $\overline{u'v'}$, is presented in Figure 3.4.

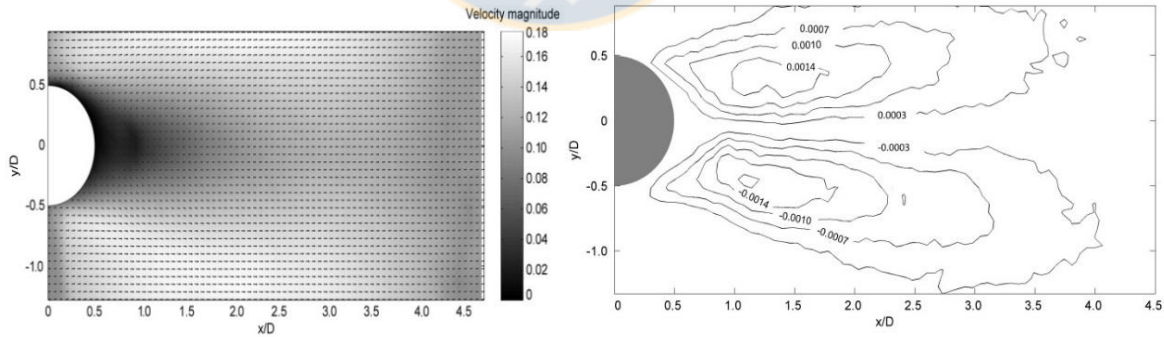


Figure 3.4 Mean velocity magnitude (left) and normalized Reynolds stresses (right) for experiment S3-19

By means of the normal stresses, the Turbulent Kinetic Energy, TKE can be approximated. For two velocity components:

$$k = 1/2 \left(\overline{(u')^2} + \overline{(v')^2} \right), \quad (3.5)$$

From the PIV measurements, time velocity-signals were extracted in the zone where the wake was fully developed. In this work and based on hydromechanics arguments, the wake is fully formed downstream the point of merging of the two separated shear layers. This position can be identified as the location of the peak of the TKE profile at the longitudinal centerline position. For example, Figure 3.5 shows the extracted profiles of TKE along the centerline for experiments S3-1, S3-7, S3-13, S3-19 and S3-25.

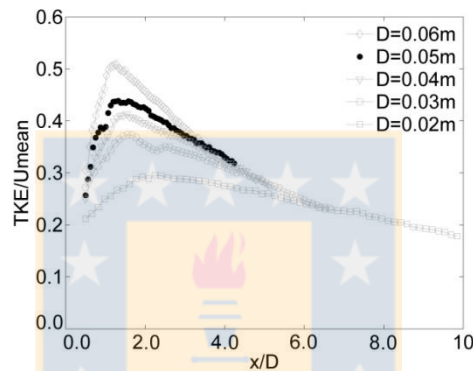


Figure 3.5 Profiles of Turbulent Kinetic Energy along the centerline for experiments S3-1, S3-7, S3-13, S3-19 and S3-25

For small diameters the distance of the TKE peak to the cylinder slightly increases. After the TKE peak almost a linear decay of the TKE with the downstream direction is observed, which occurs as a consequence of the diffusion of the wake vortices, or in other words occurs as a consequence of the processes responsible of recovering the channel flow condition.

The Strouhal number, $St = fD/U$ where f is the shedding frequency and can be properly estimated from the time series. Since the length-scales of interest are mainly large scales structures, it is expected that an estimation of f based on a Fourier analysis will accurately allow the calculation of St . Time series of the spanwise velocity component were extracted from the PIV measurements and the velocity power spectra, $E_v(f)$ was calculated for each experiment, to identify the energy peak corresponding to the vortex shedding frequencies. The power spectra can be calculated as the Fourier transform of the autocorrelation function $R_v(\tau)$:

$$E_v = 1/2\pi \int_{-\infty}^{\infty} e^{-if\tau} R_v(\tau) d\tau, \quad (3.6)$$

$$R_v(\tau) = \overline{v'(x, t)v'(x, t + \tau)}, \quad (3.7)$$

The method of Welch (1967) as implemented in the signal processing toolbox of MATLAB® was used for the calculations. Figure 3.6 show an example of a calculated autocorrelation function and the corresponding velocity spectra.

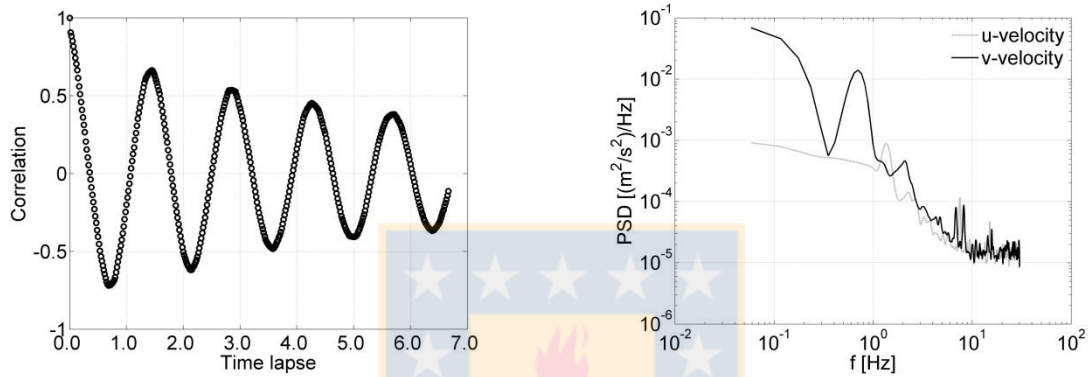


Figure 3.6 Calculated autocorrelation function (left) and power spectral density (right) for experiment S3-19

From Figure 3.6 it is possible to estimate the normalized integral time scale of the flow, about 0.35, and the spectral peak frequency, of 0.7 Hz. The presence of a spectral peak associated to the wake is evident.

3.8 Conclusions

In this chapter, the experimental setup configuration was defined. *Cheirodon galusdae* and *Basilichthys microlepidotus* were chosen as studied species of the research. Experimental series consist on testing six individuals of each species swimming in free flow and on the wake of five circular cylinders with different diameters in an open channel flow, meaning a total of seventy-two experiments. Two-dimensional Particle Image Velocimetry was chosen as the technique to measure the flow at an horizontal plane, and its physical components (*i.e.*, camera, particles and

illumination) were defined. Digital video recording of fish motion was chosen as measurement technique to quantify fish performance and tail beat movement.

To describe flow characteristics, it was decided to measure length-scale and frequency of the vortices on each experiment. Also, to describe fish motion, it was decided to realize two different measurements; fish trajectory tracking presented as a probability density function and, the description of the amplitude and frequency of the tail movement



CHAPTER 4 FISH MOTION RESULTS

4.1 Introduction

The results of fish motion study are presented below. First, a description of the behavior of studied species on the circular cylinder wake supported with a probability density function analysis of their position on the flume. Secondly, the performance of tail motion is analyzed in terms of amplitude, frequency and Strouhal number related with vortex length-scale and frequency on a dimensionless way. Finally, a discussion of the results and their possible implications on fishway design is presented.

4.2 Fish behavior

Figure 4.1 shows pictures of a fish describing a typical trajectory in the cylinder wake for *B. microlepidotus* (top, left) and *C. galusdae* (top, right), and the corresponding PDFs of the observed longitudinal (bottom, left) and transversal (bottom, right) fish positions downstream of the cylinder for experiments S3-24 for *B. microlepidotus*, and S2-20 and S2-22 for *C. galusdae*. Pictures were taken every 0.16 s during a 5.5 s long time interval and mounted in a single image.

Unlike free flow behavior, where both species just swam against the current, vortex shedding on the wake induced fishes to perform lateral movements to avoid confronting vortices frontally, as illustrated on Figure 4.1. *C. galusdae* seemed stress and so, they swam upstream to avoid the wake, being destabilized at times by bigger length-scale vortices. Whereas, *B. microlepidotus* showed comfortable swimming permanently on the wake, they kept its longitudinal position while moving laterally to avoid confronting the vortices.

The longitudinal distance covered by *C. galusdae* was significantly larger than *B. microlepidotus*. Instead, the lateral distance covered by both species was similar, they made lateral movements bigger than free flow but only the necessary to avoid confronting frontally the vortices.

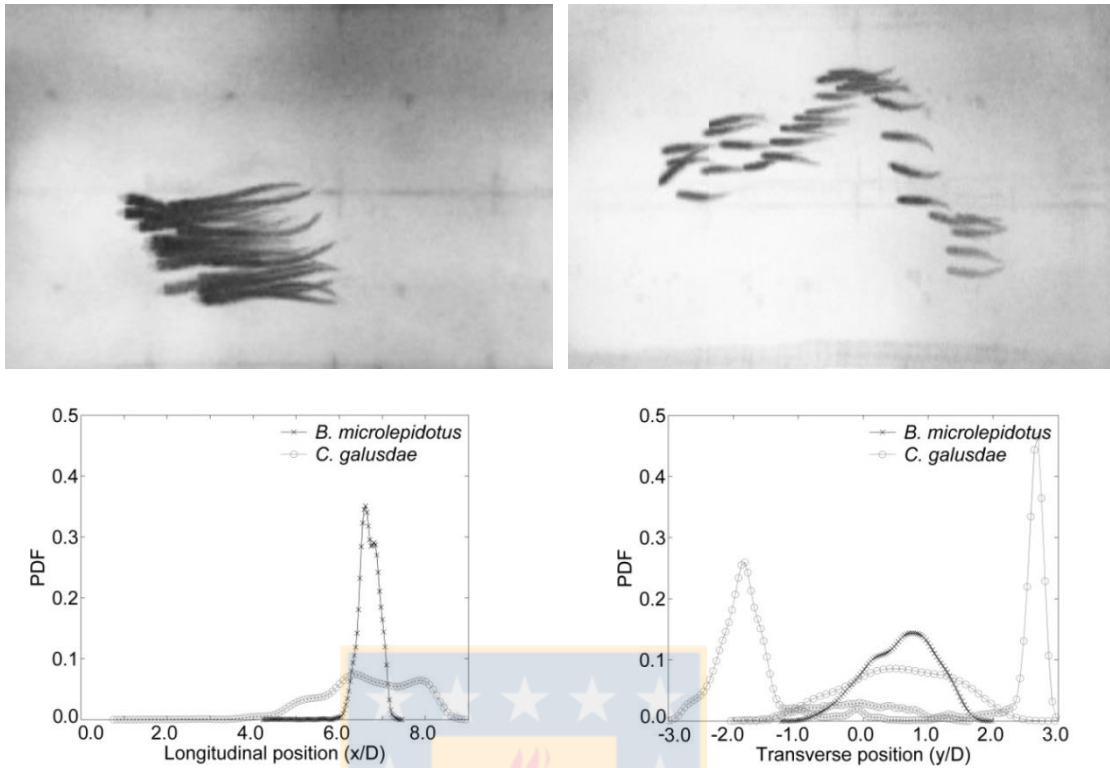


Figure 4.1 Pictures of a fish describing a typical trajectory in the cylinder wake

To ensure that the observed changes were not influenced by fish fatigue, tail beat measurements were performed at the beginning and at the end of the test showing no trends, ruling out this possibility, and attributing the changes observed on fish motion to the properties of the vortices.

4.3 Tail beat amplitude, λ

Figure 4.2 shows tail beat amplitude over relative vortex size and vortex frequency. λ is the tail beat amplitude, λ^∞ is the observed tail beat amplitude of each individual in the reference series S1, with free flow, and λ^* is the tail beat amplitude relative to the fish length. Gray dashed lines indicate the free flow condition for reference. Black, solid lines show the observed tendencies.

Individuals in the cylinder wake increased the tail beat amplitude respect to the free flow case, up to 55%. Tail beat amplitude ranged between 0.16 and 0.37 times the fish length. Relative tail beat amplitude λ^* (normalized with the fish length, $\lambda^* = \lambda / L$) of both species increased with the

relative vortex size D^* (normalized with the fish length, $D^* = (U/f) / L$) following a potential relationship $\lambda^* = aD^{*b}$ ($a=0.180$, $b=0.296$, $R^2=0.561$, $p<0.001$), and decreased linearly with vortex frequency f , following $\lambda^* = m + nf$ ($m=0.337$, $n=-0.039$, $R^2=0.371$, $p<0.001$ for *C. galusdae*; $m=0.271$, $n=-0.043$, $R^2=0.464$, $p<0.001$ for *B. microlepidotus*). Slope of the tendency line was nearly the same for both species.

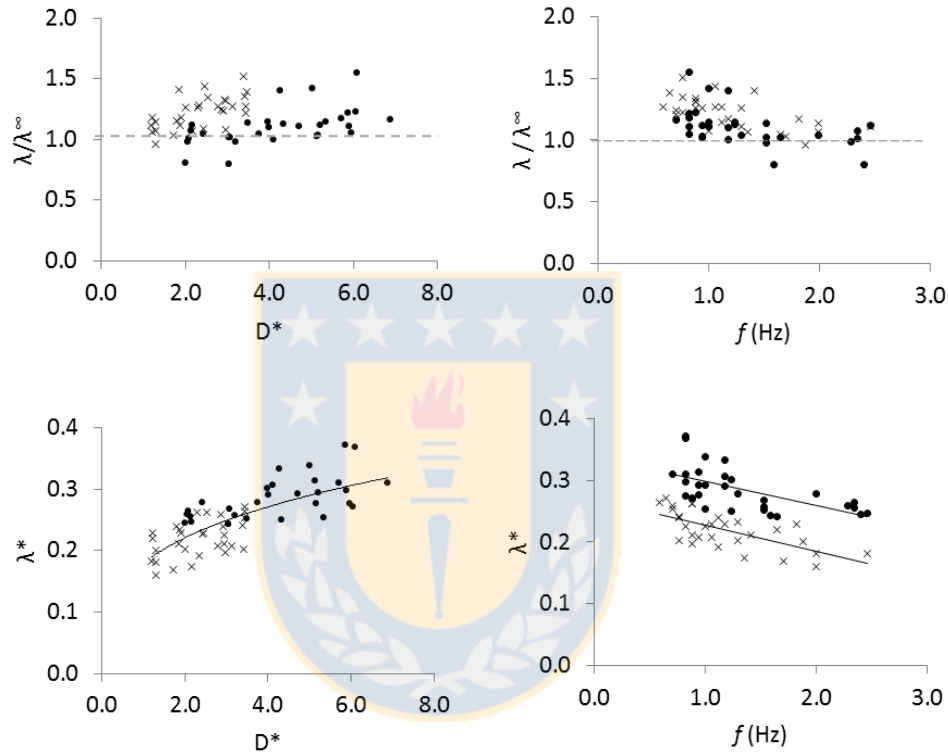


Figure 4.2 Normalized tail beat amplitude over relative vortex size (D^*) and vortex frequency (f) for experiments of series S2 (dots) and S3 (cross)

4.4 Tail beat frequency, f_{TB}

Figure 4.3 shows tail beat frequency over relative vortex size and vortex frequency. f_{TB}^∞ is the observed tail beat frequency of each individual in the reference series S1, with free flow. Gray dashed lines indicate the free flow condition for reference. Black, solid lines show the observed tendencies.

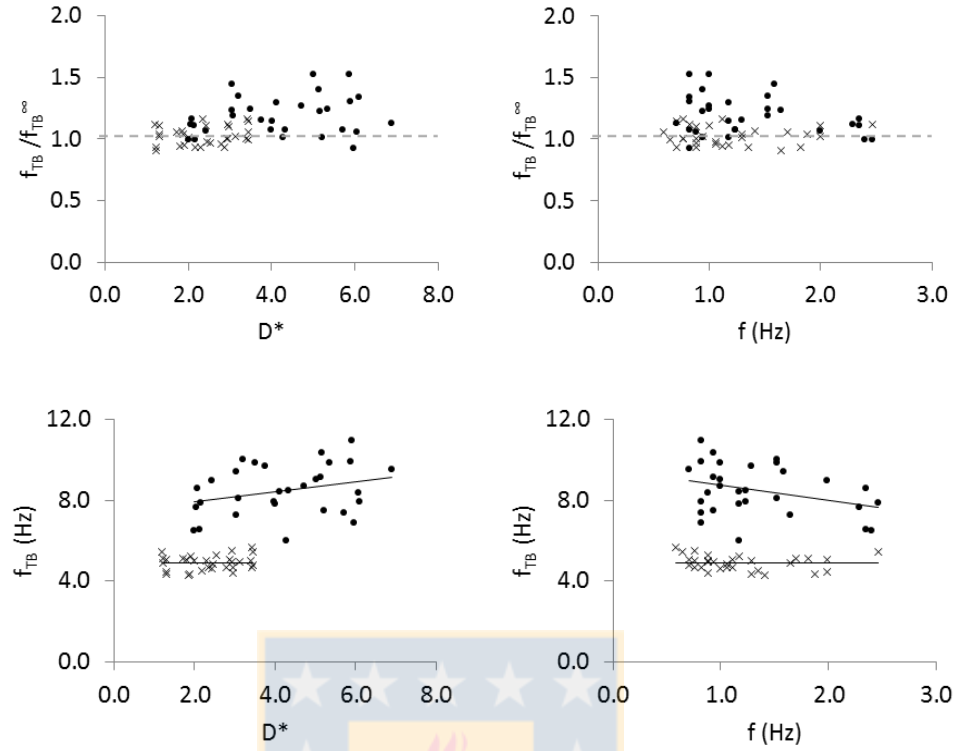


Figure 4.3 Tail beat frequency, f_{TB} over relative vortex size (D^*) and vortex frequency (f) for experiments of series S2 (dots) and S3 (cross)

Cheirodon galusdae in the cylinder wake increased the tail beat frequency compared to the free flow case, up to 52%. Tail beat frequency ranged between 6 and 11 Hz, increasing with the relative vortex size D^* following a linear relationship $f_{TB} = m + nD^*$ ($m=7.439$, $n=0.246$, $R^2=0.084$, $p=0.119$), and decreased linearly with vortex frequency f , following $f_{TB} = m + nf$ ($m=9.46$, $n=-0.731$, $R^2=0.107$, $p=0.077$). By the contrary, *B. microlepidotus* in cylinder wakes did not change the tail beat frequency observed in the free flow case of $f_{TB} = 4.9$ Hz.

Also, it was mentioned before that *C. galusdae* performs the burst-and-coast swimming style, and it was observed that ‘resting’ phase time duration decreased by 40% on average, when comparing the free flow with the six centimeters cylinder fish performance. Therefore, it is reasonable to say that *C. galusdae* tail beat frequency change is highly influenced by this.

4.5 Fish Strouhal number, St_{fish}

Figure 4.4 shows the fish Strouhal number over the relative vortex size and vortex frequency. St_{fish}^{∞} is the observed fish Strouhal number of each individual in the reference series S1, with free flow. Gray dashed lines indicate the free flow condition for reference. Black, solid lines show the observed tendencies.

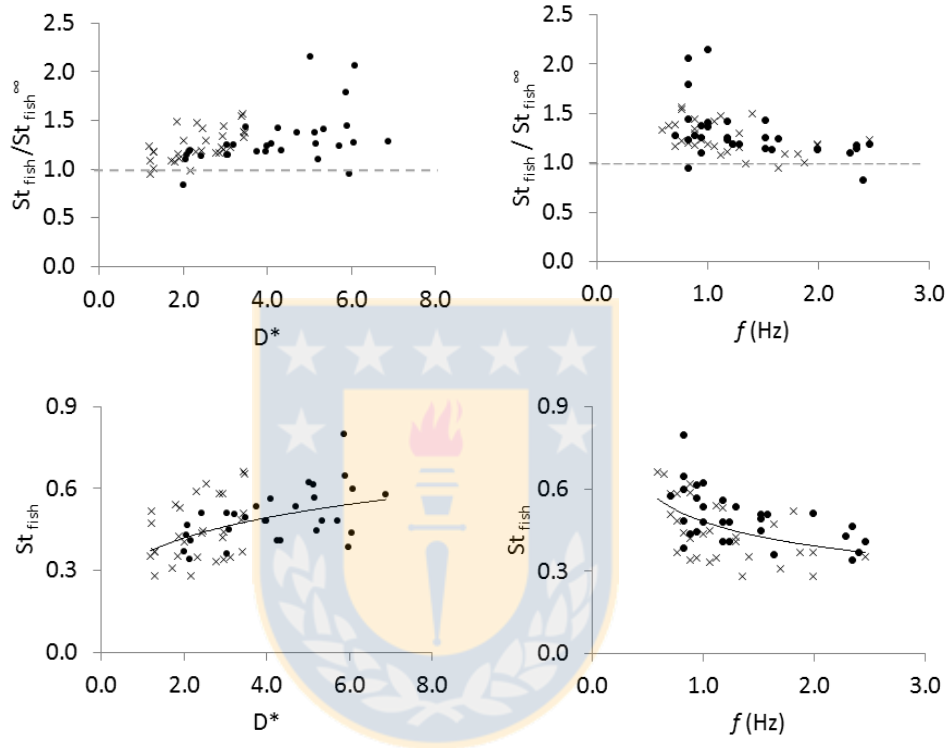


Figure 4.4 Fish Strouhal number, St_{fish} over relative vortex size (D^*) and vortex frequency (f) for experiments of series S2 (dots) and S3 (cross)

The fish Strouhal number St_{fish} of individuals in the cylinder wakes was up to 2.15 times higher than in the free flow case. St_{fish} ranged from 0.28 to 0.80. For both species St_{fish} increased with the relative vortex size D^* following a potential relationship ($a=0.356$, $b=0.235$, $R^2=0.232$, $p<0.001$), and decreased with vortex frequency f , following a potential relationship $\lambda^* = aD^{*b}$ ($a=0.481$, $b=-0.296$, $R^2=0.248$, $p<0.001$). St_{fish} proved to represent well the information on tail beat kinematics for both species. Neither a significant correlation of St_{fish} with the cylinder Reynolds number Re_D nor with the flow Strouhal number St was observed ($p = 0.147$ and $p = 0.304$, respectively).

4.6 Discussion

Upstream passage through a fishway, and thus its efficiency, importantly depends on proper stimuli for fish swimming along the fishway. Obstacles such as cylinders placed in the flow field create wakes that might stimulate fishes to swim upstream, depending on their capacity for negotiating the turbulence coherent structures. Behavior of fish species in turbulence have been scarcely studied, being Rainbow trout the most studied case (Liao *et al.*, 2003a; Liao *et al.*, 2003b; Liao, 2007; Akanyeti and Liao, 2013). This species has shown to capture energy from vortices generated by the environment diminishing the energy consumption during swimming (Taguchi and Liao, 2011). Therefore, in this study we analyze wakes as stimuli to enhance upstream passage in fishways.

For non-sport fishes, multispecies fishways appears as the best solution for providing longitudinal connectivity, nevertheless further development of fish passes technology is needed (Link and Habit, 2015; Laborde *et al.*, 2016). Development of design criteria of passes for these small body size fish is especially challenging, since they typically do not exhibit migration patterns and consequently, in a channel flow as occurring in fishways, they would just keep their position, but they would hardly swim in a desired direction such as to the pass outlet. In this context, cylinder-like obstacles appear as promising fishway elements to enhance upstream passage. However, our results showed that cylinder wakes could be favorable for upstream passage only for some species, and deleterious in other cases. In particular, *C. galusdae* behaved similar to Rainbow trout in the sense that wake vortices stimulated its movement in the upstream direction although, in this case, to escape from vortices. By the contrary, *B. microlepidotus*, did not favorable use of cylinder wakes for upstream passage, but seemed comfortable swimming on the wake. In consequence, even though we studied two non-sport species that coexist in similar habitats, and exhibit similar swimming capacities (Laborde *et al.*, 2016), their behavior in wakes was different.

Differences in the lateral line system could explain the different behavior found between the two species. The lateral line is a sensory system that allows fishes to detect weak water motions and pressure gradients, given them a refined ability to sense and respond to their fluid environment

(Bleckmann and Zelick, 2009; Liao, 2007). Hence, its development in each species is crucial for understanding the behavior in a wake (Liao, 2006; Zhang *et al.*, 2013). The basic arrangement of the lateral line system is a single branch running the length of the body trunk and splitting into several branches near the head, like in Rainbow trout (Ristroph *et al.*, 2015). Unfortunately, this sensory system has not been described in detail for neither of the two studied species. However, characiforms as *C. galusdae* are characterized by a complete lateral line, while silversides of the family Atherinopsidae, like *B. microlepidotus*, has been described with a not complete (Chernoff, 2002) or weak (Vásquez-Yeomans, 2005) lateral line, and even as absent in the trunk (Hastings *et al.*, 2014). This is a fundamental biological difference between the two studied species, and should be further analyzed in future investigations.

Numerous studies have shown a positive correlation between swimming velocity and oxygen consumption (Brett, 1964; Brett, 1965; Smit, 1965) and between swimming velocity and tail beat frequency (Bainbridge, 1958; Hunter and Zweifel, 1971; Herskin and Steffensen, 1998). Bainbridge (1958) introduced the idea that the swimming speed of a fish depends on the distance covered per tail beat cycle (the stride length, herein called tail beat amplitude) and the tail beat frequency. Bainbridge (1958) showed that tail beat amplitude and the maximum frequency were dependent on body length. The amplitude reached a maximum and could be expressed as a constant fraction of the body length at more than five tail beats per second. Hunter and Zweifel (1971) found tail beat amplitude at moderate-to-high flow speeds to be a constant fraction of body length for different sizes within each species, but tail beat amplitude varied between species. An increase in tail beat amplitude and frequency should increase the amount of thrust produced (Bainbridge, 1958; Plaut, 2002), and therefore, the ability for steady swimming. In this study, *C. galusdae* was stimulated by the wake vortices to swim upstream to avoid the stress it causes on them, tail beat frequency and amplitude was higher than in the undisturbed flow, revealing higher energy consumption in a wake. This is different than for Rainbow trout, which adapts its body shape and uses its pectoral muscles, reducing the energy costs of swimming in wakes (Liao *et al.*, 2003a). On the other side, *B. microlepidotus* did not swim upstream, and in the wake exhibited tail beat amplitudes higher than in the undisturbed flow, and thus a higher energy consumption.

Although cylinder wakes represent a special case of turbulence which is significantly different to the free flow turbulence due to the periodicity and location of the vortices, it is a two-dimensional case with homogeneous properties along the water column. Obstacles with different shapes however produce wakes with more complex vortices. In fish ramps, submerged boulders produce wakes with a marked three-dimensional shape (Bretón *et al.*, 2013; Baki *et al.*, 2014) and less periodicity. Therefore, in comparison to the cylinder case, a wake at a submerged boulder is thought less predictable for a fish. Further research is needed in order to elucidate if more complex wakes would stimulate in similar form the fish behavior. Nevertheless our results provide a first insight onto a promising alternative for efficient multispecies fish passes.

4.7 Conclusions

Results showed that both species avoid confronting frontally with vortices and interact with the wake but in different ways. *Cheirodon galusdae* seemed stress by the vortices and swam upstream to avoid them; instead, *Basilichthys microlepidotus* kept its longitudinal position swimming comfortably on the wake while moving laterally to avoid the vortices impingement.

Compared to the undisturbed flow tail beat amplitude increased in the presence of the cylinder wake. Tail beat amplitude, relative to fish length, increased with the length-scale of the vortices and decreased with their frequency. Tail beat frequencies of *C. galusdae* increased with vortices length-scale and decreased with frequency (presumably because of the shortest 'resting' time phase on the burst-and-coast swimming), while the frequencies of *B. microlepidotus* were constant in all experiments. Fish Strouhal number, defined in terms of the tail beat amplitude and frequency, correlated with the ratio between vortex length-scale and fish length ratio for both species. It is concluded that wakes might serve as attraction flow and stimuli for upstream passage of *C. galusdae* and, *B. microlepidotus* would not favorable use cylinder wakes in a fishway.

CHAPTER 5 CONCLUSIONS

The behavior and tail beat kinematics of two non-sport fish species from Chile, *C. galusdae* and *B. microlepidotus* juveniles, in the wake of a vertical and bottom-mounted circular cylinder in an open channel flow were studied through two-dimensional PIV and digital video of fish motion.

Results show that both species avoid vortices impingement and interact with the wake differently. *C. galusdae* seemed stress and swam upstream escaping from vortices while, *B. microlepidotus* swam on the wake and kept its longitudinal position while moving laterally to avoid confronting vortices.

Compared to free flow, tail beat amplitude increased in the presence of the wake. Tail beat amplitude, relative to fish length, increased with the length-scale of the vortices and decreased with their frequency. Tail beat frequencies of *C. galusdae* increased with vortices length-scale and decreased with frequency presumably because of the shortest resting time phase on the burst-and-coast swimming, while the tail beat frequencies of *B. microlepidotus* were constant in all experiments. Fish Strouhal number, defined in terms of the tail beat amplitude and frequency correlated with the ratio between vortex length-scale and fish length ratio for both species.

Wakes might serve as stimuli for upstream passage of *C. galusdae*, while *B. microlepidotus* would not favorable use cylinder wakes for upstream passage in a fishway and showed attraction for swimming on cylinder wake. Compared to the undisturbed flow condition, they would exhibit higher energy consumption under such conditions.

Because this research was planned as a unique problem, some of its limitations should be investigated in future works. Bigger sample size, a different turbulence structure configuration with different cylinder diameters or straightforward changing the cylinder with a boulder arrangement, further research on the energetics of non-sport fish swimming in altered flows, e.g. respirometry, further study about fish tracking concerning velocity and acceleration changes are some of the ideas that would contribute to achieve a biggest understanding and knowledge about this new research topic.

REFERENCES

Adrian, R., and J. Westerweel (2011). **Particle Image Velocimetry**. Cambridge University Press. Cambridge.

Akanyeti, O., and J. Liao (2013). A kinematic model of Kármán gaiting in rainbow trout. **Journal of Experimental Biology**. **216(24)**. 4666-4677.

Bainbridge, R. (1958). The speed of swimming of fish as related to size and to the frequency and amplitude of the tail beat. **Journal of experimental biology**. **35(1)**. 109-133.

Baki, A., D. Zhu and N. Rajaratnam (2014). Turbulence characteristics in a rock-ramp-type fish pass. **Journal of Hydraulic Engineering**. **141(2)**. 040140751-0401407512.

Bleckmann, H. and R. Zelik (2009). Lateral line system of fish. **Integrative Zoology**. **4(1)**. 13-25.

Bretón, F., A. Baki, O. Link, D. Zhu and N. Rajaratnam (2013). Flow in nature-like fishway and its relation to fish behaviour. **Canadian Journal of Civil Engineering**. **40(6)**. 567-573.

Brett, J. (1964). The respiratory metabolism and swimming performance of young sockeye salmon. **Journal of the Fisheries Board of Canada**. **21(5)**. 1183-1226.

Brett, J (1965). The relation of size to rate of oxygen consumption and sustained swimming speed of sockeye salmon (*Oncorhynchus nerka*). **Journal of the Fisheries Board of Canada**. **22(6)**. 1491-1501.

Castro-Santos, T., A. Cotel and P. Webb (2009). Fishway evaluations for better bioengineering: an integrative approach. **Proceedings of the International Symposium "Challenges for Diadromous Fishes in a Dynamic Global Environment"**. Halifax, Nova Scotia. Canada. June.

Chernoff, B. (2002). Order Atheriniformes. In K. Carpenter (ed.) **The living marine resources of the Western Central Atlantic. Volume 2: Bony fishes part 1 (Acipenseridae to Grammatidae)**. FAO Species Identification Guide for Fishery Purposes and American Society of Ichthyologists and Herpetologists Special Publication No. 5. Rome.

Dermisis, D., and A. Papanicolaou (2009). Fish passage over hydraulic structures in Midwestern Rivers of the USA. **International Journal of River Basin Management**. **7(4)**. 313-328.

Dyer, B. (2000). Systematic review and biogeography of the freshwater fishes of Chile. **Estudios Oceanológicos**. **19**. 77-98.

Enders, E., D. Boisclair and A. Roy (2003). The effect of turbulence on the cost of swimming for juvenile Atlantic salmon (*Salmo salar*). **Canadian Journal of Fisheries and Aquatic Sciences**. **60(9)**. 1149-1160.

Fey, U., M. König and H. Eckelmann (1998). A new Strouhal-Reynolds-number relationship for the circular cylinder in the range $47 < Re < 2 \times 10^5$. **Physics of Fluids**. **10(7)**. 1547-1549.

García, A., C. Sobenes, O. Link and E. Habit (2012). Bioenergetic models of the threatened darter *Percilia irwini*. **Marine and Freshwater Behavior and Physiology**. **45(1)**. 17-28.

Goettel, M., J. Atkinson and S. Bennett (2015). Behavior of western blacknose dace in a turbulence modified flow field. **Ecological Engineering**. **74**. 230-240.

Gross, D., W. Brevis and G. Jirka (2010). Development of a LED-based PIV/PTV system: Characterization of the flow within a cylinder wall-array in a shallow flow. **Proceedings of the International Conference on Fluvial Hydraulics River Flow 2010**. Braunschweig, Germany. September

Hastings, P., H. Walker and G. Galland (2014). **Fishes: a Guide to their Diversity**. University of California Press. Oakland.

Herskin, J., and J. Steffensen (1998). Energy savings in sea bass swimming in a school: measurements of tail beat frequency and oxygen consumption at different swimming speeds. **Journal of Fish Biology**. **53(2)**. 366-376.

Hunter, J., and J. Zweifel (1971). Swimming speed, tail beat frequency, tail beat amplitude, and size in jack mackerel, *trachurus-symmetricus*, and other fishes. **Fishery Bulletin of the National Oceanic and Atmospheric Administration**. **69(2)**. 253-266.

Jobling, M. (1982). Some observations on the effects of feeding frequency on the food intake and growth of plaice, *Pleuronectes platessa* L. **Journal of Fish Biology**. **20(4)**. 431- 444.

Laborde, A., A. González, C. Sanhueza, P. Arriagada, M. Wilkes, E. Habit and O. Link (2016). Hydropower development, riverine connectivity and nonsport fish species: Criteria for hydraulic design of fishways. **River Research and Applications**. **2016**.

Lacey, R., V. Neary, J. Liao, E. Enders and H. Tritico (2012). The IPOS framework: linking fish swimming performance in altered flows from laboratory experiments to rivers. **River Research and Applications**. **28(4)**. 429-443.

Liao, J., D. Beal, G. Lauder and M. Triantafyllou (2003a). The Kármán gait: novel body kinematics of rainbow trout swimming in a vortex street. **Journal of experimental biology**. **206(6)**. 1059-1073.

Liao, J., D. Beal, G. Lauder and M. Triantafyllou (2003b). Fish exploiting vortices decrease muscle activity. **Science**. **302(5650)**. 1566-1569.

Liao, J. (2006). The role of the lateral line and vision on body kinematics and hydrodynamic preference of rainbow trout in turbulent flow. **Journal of Experimental Biology**. **209(20)**. 4077-4090.

Liao, J. (2007). A review of fish swimming mechanics and behavior in altered flows. **Philosophical Transactions of the Royal Society**. **362**. 1973-1993.

Link, O. and E. Habit (2015). Requirements and boundary conditions for fish passes of non-sport fish species based on Chilean experiences. **Reviews in Environmental Science and Bio/Technology**. **14(1)**. 9-21.

Lupandin, A. (2005). Effect of flow turbulence on swimming speed of fish. **Biology Bulletin**. **32(5)**. 461-466.

Maia, A., A. Sheltzer and E. Tytell (2015). Streamwise vortices destabilize swimming bluegill sunfish (*Lepomis macrochirus*). **The Journal of experimental biology**. **218(5)**. 786-792.

Melling, A. (1997). Tracer particles and seeding for particle image velocimetry. **Measurement Science and Technology**. **8(12)**. 1406–1416.

Ministerio de Energía (2015). **Base para Planificación Territorial en el Desarrollo Hidroeléctrico Futuro**. Chilean Ministry of Energy. Santiago.

Myers, N., R. Mittermeier, C. Mittermeier, G. Da Fonseca and J. Kent (2000). Biodiversity hotspots for conservation priorities. **Nature**. **403(6772)**. 853-858.

Nikora, V., J. Aberle, B. Biggs, I. Jowett and J. Sykes (2003). Effects of fish size, time-to-fatigue and turbulence on swimming performance: a case study of *Galaxias maculatus*. **Journal of Fish Biology**. **63(6)**. 1365-1382.

Otsu, N. (1979). An automatic threshold selection method based on discriminate and least squares criteria. **Denshi Tsushin Gakkai Ronbunshi**. **63**. 349-356.

Oufiero, C., K. Jugo and T. Garland (2014). Swimming with a sword: tail beat kinematics in relation to sword length in *Xiphophorus*. **Functional Ecology**. **28(4)**. 924-932.

Plaut, I. (2002). Does pregnancy affect swimming performance of female Mosquitofish, *Gambusia affinis*?. **Functional Ecology**. **16(3)**. 290-295.

Ristroph, L., J. Liao and J. Zhang (2015). Lateral line layout correlates with the differential hydrodynamic pressure on swimming fish. **Physical review letters**. **114(1)**. 0181021-0181025.

Russon, I. and P. Kemp (2011). Advancing provision of multi-species fish passage: behaviour of adult European eel (*Anguilla anguilla*) and brown trout (*Salmo trutta*) in response to accelerating flow. **Ecological Engineering**. **37(12)**. 2018-2024.

Scarano, F. (2001). Iterative image deformation methods in PIV. **Measurement science and technology**. **13(1)**. R1-R19.

Schlichting, H. and K. Gersten (1997). **Boundary-Layer Theory**. Springer Science & Business Media. Berlin.

Shao, X., D. Pan, J. Deng and Z. Yu (2010). Hydrodynamic performance of a fishlike undulating foil in the wake of a cylinder. **Physics of Fluids**. **22(11)**. 1119031-1119039.

Smit, H. (1965). Some experiments on the oxygen consumption of goldfish (*Carassius auratus* L.) in relation to swimming speed. **Canadian Journal of Zoology**. **43(4)**. 623-633.

Sobenes, C., A. García, E. Habit and O. Link (2012). Mantención de Peces Nativos Dulceacuícolas de Chile en cautiverio: un aporte a su conservación ex situ. **Boletín de Biodiversidad de Chile**. **7**. 27-41.

Taguchi, M. and J. Liao (2011). Rainbow trout consume less oxygen in turbulence: the energetics of swimming behaviors at different speeds. **The Journal of experimental biology**. **214(9)**. 1428-1436.

Tennekes, H. and J. Lumley (1972). **A First Course in Turbulence**. MIT press. Cambridge.

Thielicke, W. and E. Stamhuis (2014a). PIVlab – Towards User-friendly, Affordable and Accurate Digital Particle Image Velocimetry in MATLAB. **Journal of Open Research Software**. **2(1)**. e30 1-10.

Thielicke, W. and E. Stamhuis (2014b). **PIVlab - Time-Resolved Digital Particle Image Velocimetry Tool for MATLAB (version 1.41)**.

Tritico, H. and A. Cotel (2010). The effects of turbulent eddies on the stability and critical swimming speed of creek chub (*Semotilus atromaculatus*). **The Journal of experimental biology**. **213(13)**. 2284-2293.

Vásquez-Yeomans, L. (2005). Atherinopsidae: New world silversides. In W. Richards (ed.). **Early life stages of Atlantic fishes: an identification guide for the western central North Atlantic**. CRC Press. Boca Raton.

Véliz, D., L. Catalán, R. Pardo, P. Acuña, A. Díaz, E. Poulin and I. Vila (2012). El género *Basilichthys* (Teleostei: Atherinopsidae) analizado a lo largo de su distribución en Chile (21° a 40° S), utilizando rasgos morfológicos y variabilidad del ADN mitocondrial. **Revista chilena de historia natural**. **85(1)**. 49-59.

Videler, J. and C. Wardle (1991). Fish swimming stride by stride: speed limits and endurance. **Reviews in Fish Biology and Fisheries**. **1(1)**. 23-40.

Vila, I. and E. Habit (2015). Current situation of the fish fauna in the Mediterranean region of Andean river systems in Chile. **Fishes in Mediterranean Environments**. **2015(2)**. 1-19.

Welch, P. (1967). The use of fast Fourier transform for the estimation of power spectra: A method based on time averaging over short, modified periodograms. **IEEE Transactions on audio and electroacoustics**. **15(2)**. 70-73.

Westerweel, J. and F. Scarano (2005). Universal outlier detection for PIV data. **Experiments in Fluids**. **39(6)**. 1096-1100.

Williamson, C. (1996). Vortex dynamics in the cylinder wake. **Annual review of fluid mechanics**. **28(1)**. 477-539.

Zarfl, C., A. Lumsdon, J. Berlekamp, L. Tydecks and K. Tockner (2015). A global boom in hydropower dam construction. **Aquatic Sciences**. **77(1)**. 161-170.

Zhang, J., L. Ristroph and J. Liao (2013). The lateral line system of fish as a hydrodynamic antenna. **Bulletin of the American Physics Society**. **58(18)**. 17002.

